Chapter 3

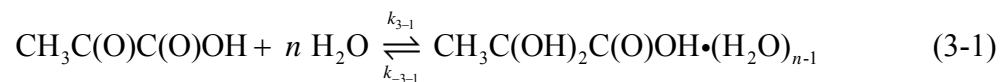# Cooperative Hydration of Pyruvic Acid in Ice

Abstract

About 3.5 ± 0.3 water molecules are still involved in the exothermic hydration of 2-oxopropanoic acid (pyruvic acid, PA) into 2,2'-dihydroxypropanoic acid (PAH) in ice at 230 K. Thermodynamics, and the fact that $Q_H(T) = [PAH]/[PA]$ becomes temperature independent below ~ 250 K (in chemically and thermally equilibrated frozen $0.1 \leq [PA]/M \leq 4.6$ solutions in D_2O), requires that the enthalpy of PA hydration (ΔH_H ~ -22 kJ mol^{-1}) be balanced by a multiple of the enthalpy of ice melting (ΔH_M = 6.3 kJ mol^{-1}). Considering that: (1) thermograms of frozen PA solutions display a single endotherm, at the onset of ice melting, (2) the sum of the integral intensities of the $^1\delta_{PAH}$ and $^1\delta_{PA}$ methyl proton NMR resonances remains nearly constant and, (3) bandwidths display an inverse temperature dependence before diverging below ~ 230 K, we infer that PA is cooperatively hydrated while dissolved in increasingly viscous aqueous microfluids down to vitrification.

Introduction

The fluid films wetting ice supports important chemical, biochemical, and environmental processes.[1-7] The existence of subeutectic aqueous solutions;[8-10] of unfrozen water bound to mesoscopic objects, such as membranes and macromolecules, in the presence of ice;[1-3,11,12] and the premelting[13-16] and prefreezing[17] of pure substances and mixtures reveal that interfaces differ significantly from bulk phases, and can support novel phenomena.

Upon freezing, solutes largely (> 99.9%) accumulate in the unfrozen portion,[6,8,18-24] but the marginal and selective incorporation of ions into ice induces sizable polarizations that are ultimately relieved by interfacial proton migration.[25-27] Chemical reaction rates and equilibria in frozen solutions are therefore expected to be enhanced by trivial concentration effects,[28] generally retarded by the prevalent low temperatures[26,29] and potentially affected by the acidity changes ensuing freezing.[30] Although solute solvation plays a crucial role in chemistry, the likelihood of water exchange and the extent of solute dehydration in ice interfacial layers, vis-a-vis the decreased activity of water at subfreezing temperatures, remains largely unexplored. The hydration of pyruvic acid (PA) into its *gem*-diol, 2,2'-dihydroxypropanoic acid (PAH), reaction (3-1):

$$CH_3C(O)C(O)OH + n\ H_2O \underset{k_{-3-1}}{\overset{k_{3-1}}{\rightleftharpoons}} CH_3C(OH)_2C(O)OH \bullet (H_2O)_{n-1} \qquad (3\text{-}1)$$

whose equilibrium constant, K_H:

$$K_H = \frac{[CH_3C(OH)_2COOH \bullet (H_2O)_{n-1}]}{[CH_3COCOOH]\, a_w^n} = \frac{Q_H}{a_w^n} \qquad (3\text{-}2)$$

(where a_w is the water activity) is known to involve more than the stoichiometric ($n = 1$) amount of water in fluid solutions,[31-35] should be a sensitive probe of water availability in frozen media.[36-39] Here we report magic angle spinning nuclear magnetic resonance (MAS NMR) and differential scanning calorimetry (DSC) experiments in fluid and frozen pyruvic acid aqueous solutions down to 230 K that provide quantitative information on the properties of the quasi-liquid layer.

Experimental Section

MAS ^{1}H-NMR spectra of frozen PA (Aldrich 98.0%, doubly distilled under vacuum) solutions in D_2O (Alfa 99.8%, $T_f = 277.0$ K), contained in capped ZrO_2 rotors (100 μL, 4 mm internal diameter) spun at 3.2 ± 0.1 kHz were acquired with a Bruker ARX500 spectrometer equipped with a triple resonance 4 mm probe and cavity temperature control. Spinning samples were allowed to equilibrate for at least 20 minutes at each temperature prior to spectral scans. Spectra were scanned over consecutive cooling and warming sequences spanning the entire temperature range, or over ± 2 K cycles about specific temperatures. Probe temperatures were calibrated using reported $^1\delta_{OH}$ - $^1\delta_{CH_3}$ vs. T data for methanol down to 228 K.[40] ^{1}H-NMR spectra of fluid solutions were recorded with a Varian Unity 500 Plus spectrometer. Structured spectral peaks were deconvoluted into single Lorentzians. Thermal studies on aqueous PA samples (200 μL) were performed in a Netzsch STA 449 differential scanning calorimeter (DSC) calibrated with neat H_2O and D_2O standards.

Results and Discussion

The ^{1}H-NMR spectra of neat PA(l) at 298 K show resonances at 8.70 ppm and 2.53 ppm (relative to TMS), which are assigned to acidic and methyl protons, respectively. The ^{1}H-NMR spectrum of PA in aqueous solution displays, in contrast, two methyl bands: one at $^1\delta$ = 1.54 ppm, which corresponds to PAH, and a less intense one, at $^1\delta$ = 2.38 ppm, the correlate of the 2.53 ppm PA band (Figure 3-1). The positions of the 1.54 and 2.38 bands of PAH and PA slightly shift upfield, while their peak intensities and widths change smoothly with decreasing temperature (Figure 3-1). A single $^1\delta$ > 5 ppm band, which markedly shifts downfield and broadens at lower temperatures (Figure 3-2), is assigned to mobile water protons,[19,41-43] arising from rapid proton exchange between [^{1}H$_4$]PA and solvent D$_2$O. The $^1\delta$ band of water held in the relatively anhydrous environment of reverse micelles is known to shift, in contrast, upfield.[42,44]

PA and PAH concentrations in aqueous solution are directly proportional to the 2.38 and 1.54 ppm band areas, respectively. Figure 3-3 shows Q_H = [PAH]/[PA] measurements as a function of a_w (standard state neat water, i.e., x_w = 1, 298 K) in aqueous PA solutions of various compositions ($0.002 \leq x_{PA} = 1 - x_w \leq 0.87$) at 298 K. The two curves in Figure 3-3 were drawn from present $Q_H(x_w)$ values by: (1) assuming a_w = x_w throughout or, (2) adopting the a_w = $a_w(x_w)$ data reported for acetic acid aqueous solutions. These choices are deemed to bracket the anticipated (positive) deviations of the water activity coefficient, γ_w = $a_w/x_w \geq 1$, in PA solutions.[45-47] The limiting slopes of the log Q_H vs. log a_w plots of Figure 3-1 at $a_w \rightarrow 0$ and $a_w \rightarrow 1$ correspond, according to Equation (3-2), to n_0 and n_1, the number of water molecules actually involved in

equilibrium (3-1, -3-1) in concentrated and dilute PA solutions, respectively. We obtain $n_0 = 0.9$, $n_1 = 6.2$ for choice (1) above, and $n_0 = 1.2$, $n_1 = 8.3$ for choice (2). These n_1 values encompass the $n_1 \sim 6.5$ value previously reported for PA hydration in water-dioxane mixtures in the range $0.6 \leq a_w \leq 1.$[32] The same report indicates strong deviations at $a_w \leq 0.6$, which are consistent with the condition $n_0 < n_1$, i.e., with decreased solvation in more concentrated PA solutions. Notice that the $n \sim 3$ values derived elsewhere from log Q_H vs. log [H_2O] plots are implicitly based on the choice of 1 M water ideal solution at 298 K as standard state,[31] which is not appropriate for correlating the Q_H vs. a_w dependences above and below the freezing point. It is the activity of pure water, i.e., a_w in the molar fraction concentration scale, that is related to the activity of ice, the stable phase, at subfreezing temperatures.

The Q_H vs. T data obtained in 0.10, 2.32 and 4.64 M PA solutions above and below their respective freezing points are shown in Figure 3-4. As expected, Q_H increases with decreasing temperature in the fluid region in all cases. We obtain $\Delta H_H = -27.3$ kJ mol^{-1} for the 0.1 M PA solution, in excellent agreement with Menzel's data in D_2O as solvent at 298 K,[35] and $\Delta H_H = -21.3$ and 20.5 kJ mol^{-1} for the 2.32 and 4.64 M PA solutions, respectively. These figures confirm that PAH stability and n increase with dilution. As a reference, the colligatively depressed freezing temperatures (estimated from the cryoscopic constant of D_2O, $\lambda = 2.01$ K molal^{-1}, by assuming that PA remains largely undissociated) are $T_f \sim 277.0 - 2.01$ [PA] = 276.8, 272.3 and 267.7 K, for [PA] = 0.10, 2.32 and 4.64 M, respectively. Although these solutions freeze without discontinuities in Q_H, the slope, $\partial Q_H / \partial T = \partial (K_1 \times a_w{}^n) / \partial T$, reverses its sign at T_f for the more dilute 0.1 M

PA solution. Ultimately, all Q_H's asymptotically merge into a common $Q_H = 4.2 \pm 0.3$ value below ~ 250 K (Figure 3-4).

There is no evidence of thermal hysteresis in these experiments. The same $Q_H(T)$ curves, within experimental precision, were obtained whether the corresponding temperatures were reached along cooling or warming sequences. The same Q_H values were recovered > 60 min after the frozen solutions had reached thermal equilibrium. Since reactions (3-1, -3-1) are known to exhibit acid catalysis in solution,[33,36] the fact that Q_H's measured in frozen acidified solutions are not significantly different (inset, Figure 3-4) supports the assumption of chemical equilibrium in the frozen state, even at the lowest temperatures. This empirical conclusion is consistent with the relaxation times $\tau <$ 100 s, for approaching equilibrium (3-1, -3-1) in aqueous $[H^+] = 0.1$ M solutions, estimated by extrapolation of available kinetic data to 250 K.[33]

These experiments show that equilibrium (3-1, -3-1) is not arrested at the freezing point, but remains dynamic down to significantly lower temperatures, despite the reduced water activity and molecular mobilities prevailing in the unfrozen solution. What prevents the complete dehydration of PAH at lower temperatures? Although a_w is a function of both x_w (Figure 3-3) and temperature in aqueous solutions, the onset of the phase equilibrium, $H_2O(l, x_w) \ \Phi \ H_2O(s)$, renders a_w an exclusive function of T below T_f, independent of the nature of the solute.[48] The activity of water in equilibrium with ice at $T \leq T_f$ can be evaluated from[14,15]

$$a_w = \exp\left[\frac{\Delta H_M}{R}\left(\frac{1}{T_f} - \frac{1}{T}\right)\right] \qquad (3\text{-}3)$$

where ΔH_M is the enthalphy of ice melting. Equation (3-3) leads, with $\Delta H_M(H_2O) = 6.01$ kJ mol^{-1}, to $a_w = 0.78$ vs. the experimental value for supercooled water $a_w = 0.80$ at 250 K.[49,50] The inverse temperature dependence of Q_H in 0.1 M PA at $T > T_f$ is retrieved from Equation (3-2) with $\Delta H_H = -27.3$ kJ mol^{-1}, $a_w \sim 1$: $Q_H = K_H \, a_w^n \propto \exp\text{-}(\Delta H_H/RT) = \exp(3284/T)$. On the other hand, n may be still approximated by $n_1 \sim 7$ just below T_f, but now a_w is given by Equation 3-3 with $\Delta H_M(D_2O) = 6.34$ kJ mol^{-1}. The expression that follows: $Q_H \propto \exp[-(\Delta H_H + n_1 \Delta H_M)/RT] = \exp[-2062/T]$, correctly predicts the reversal of $\partial Q_H/\partial T$ about T_f (Figure 3-4). In contrast with the thermal behavior of the 0.1 M PA solution, the monotonous increase of Q_H upon cooling the 4.64 M PA solution, even below its corresponding freezing point (Figure 3-4), implies that in this case, $\Delta H_H + n \, \Delta H_M \leq 0$. Thus, PA may become more or less hydrated in the frozen state, depending on the initial concentration of the fluid solution. Because $\Delta C_{p,m} \sim 0$, i.e., ΔH_M is nearly independent of temperature, the thermal behaviors of Q_H below T_f depend on the relative values of $\Delta H_H/n$ and ΔH_M.

The experimental observation that $\partial Q_H/\partial T \rightarrow 0$ as $T \rightarrow 250$ K for *all* solutions reflects, therefore, a thermodynamic rather than a kinetic condition: it actually requires that $(\Delta H_H + n \, \Delta H_M) \rightarrow 0$ in the presence of ice at low temperatures. The data of Figure 3-3 suggest that n is likely to decrease along with temperature in the increasingly concentrated solutions remaining below T_f. By assuming that $\Delta H_H \rightarrow 21.3$ kJ mol^{-1} at low temperatures (as for the 2.32 M PA solution that leads to $Q_H = 4.0$ at the onset of freezing) we arrive at the conclusion that a minimum of $n \sim 3.5 \pm 0.3$ water molecules are needed to hydrate the carbonyl group of PA in ice below ~ 255 K. This figure provides a

stringent measure of hydrogen σ-bond cooperativity as a mechanistic requisite for solute hydration under rather adverse conditions.[2,36,39,51-53]

The preceding evidence suggests that PA hydration occurs in a fluid medium down to, at least, 250 K. A rigid reaction medium would have otherwise restricted the expansion (ΔV_{3-1} = -5 × 10^{-3} L mol^{-1})[54] associated with PAH dehydration. Since the area of the $^1\delta$ > 5 ppm signals of Figure 3-2, A_w, gauges the amount of liquid water in frozen solutions,[9,43] and A_w vanishes below ~ 250 K (Figure 3-5), water seems to freeze completely at the point at which Q_H becomes independent of temperature.

On the other hand, the linewidths of methyl proton resonances, which gradually increase at lower temperatures (Figure 3-6), abruptly broaden below ~ 230 K (i.e., about 20 K below the disappearance of mobile water) as an indication that internal rotations of methyl groups become too slow to effectively average local magnetic anisotropy,[55,56] at temperatures that are commensurate with the glass transition of bulk supercooled D$_2$O, T$_g$ = 233 K.[19,57] DSC thermograms of frozen PA solutions, which display a single endotherm at the onset of ice melting (Supporting Information), further confirm that PA aqueous solutions freeze into ice and a fluid solution that eventually vitrifies at ~ 230 K.
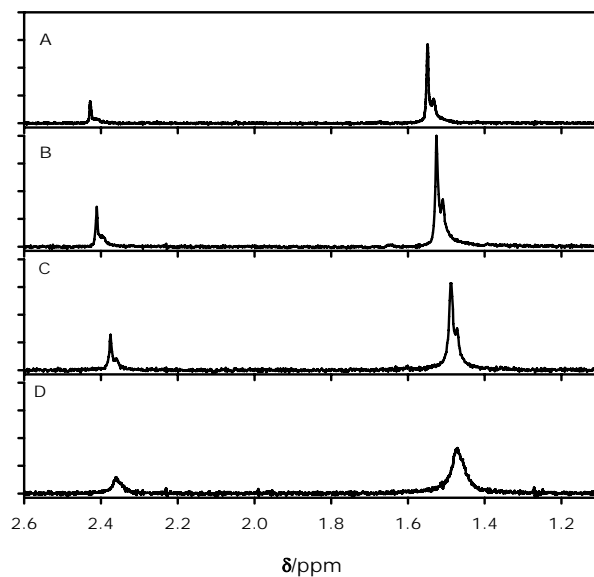
Figure 3-1. MAS ^{1}H NMR spectra of frozen 0.1 M pyruvic acid solutions in D_2O at 275.3 (**A**), 261.3 (**B**), 250.5 (**C**), and 239.7 K (**D**). Signals at $^1\delta \sim 2.4$ and ~ 1.5 ppm (vs. TMS) correspond to methyl protons of pyruvic acid and its hydrate, respectively.
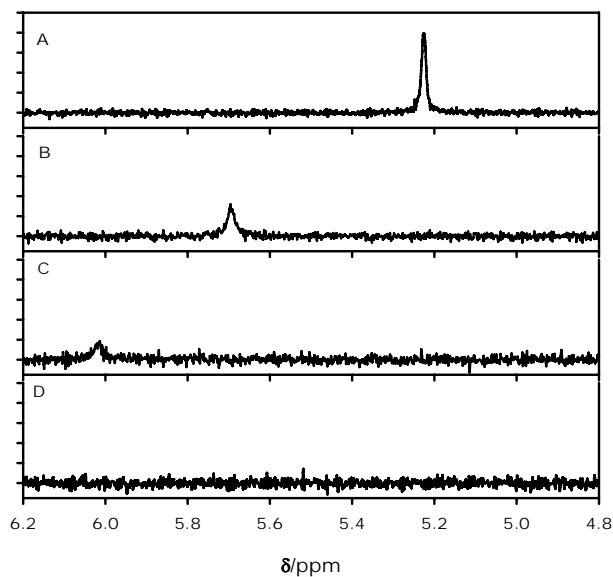

Figure 3-2. The $^1\delta \sim 5$ ppm water NMR signals in frozen 0.1 M pyruvic acid solutions in D_2O under the same conditions of Figure 3-1.
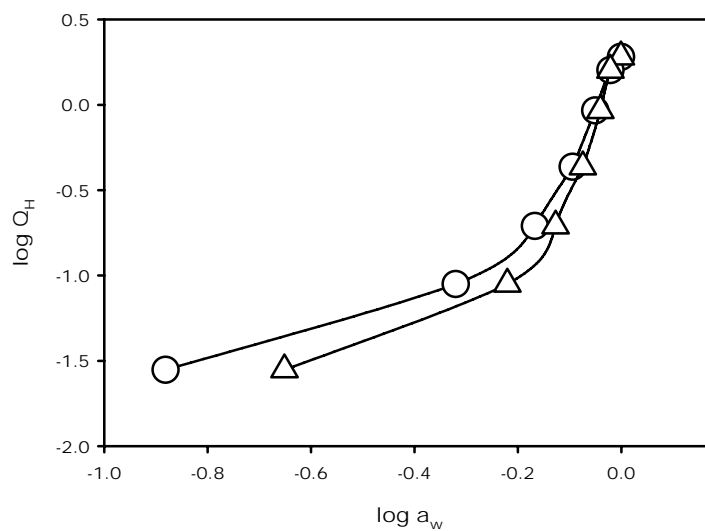
Figure 3-3. Log Q_H vs. log a_w in PA solutions in D_2O at 298 K. ($\bigcirc$) $\gamma_w = 1$. ($\triangle$) γ_w as in acetic acid solutions.[45]
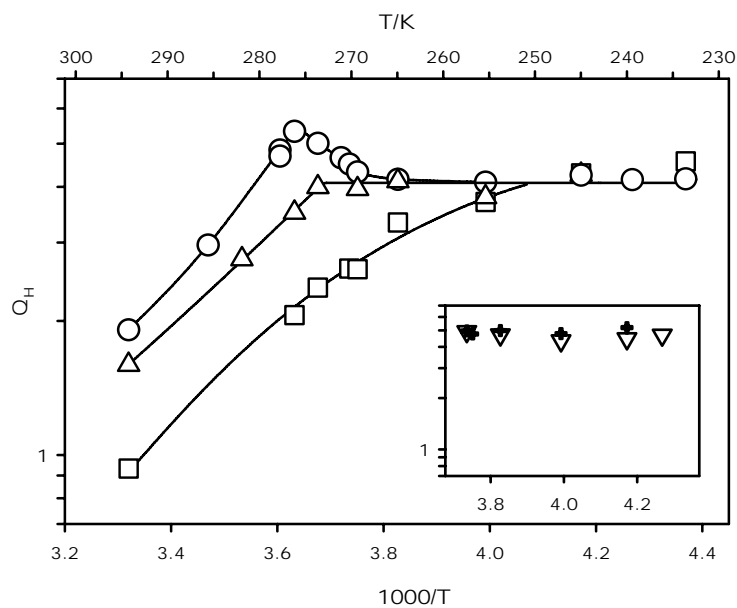
Figure 3-4. Log Q_H vs. 1000/T in: ($\bigcirc$) 0.1 M. ($\triangle$) 2.32 M. ($\square$) 4.64 M PA solutions in D_2O. Insert: ($\triangledown$) in 0.16 M PA/0.13 M HCl. ($+$) in 0.16 M PA/0.5 M NaCl.
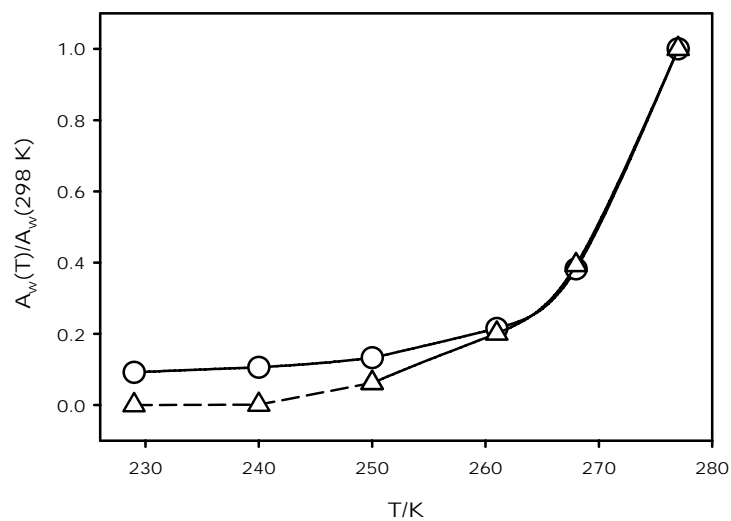
Figure 3-5. Integral intensity of the $^1\delta \sim 5$ ppm water signals as function of temperature. ($\triangle$) in 0.10 M PA. ($\bigcirc$) in 0.16 M PA/0.13 M HCl.
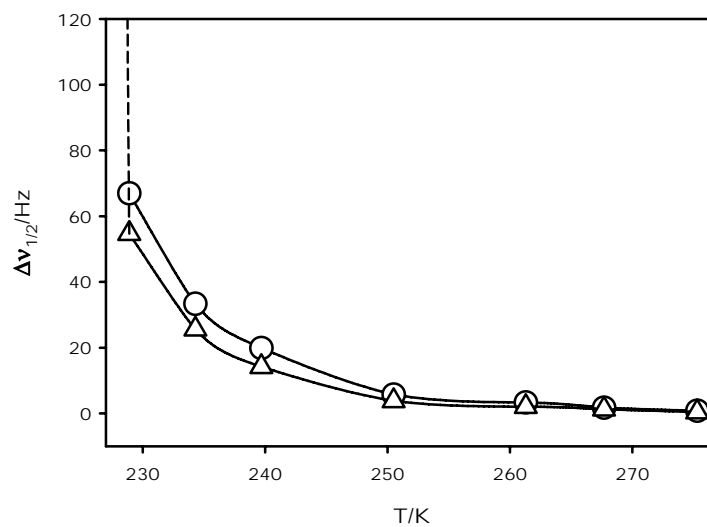

Figure 3-6. ($\bigcirc$) $^1\delta$: ~ 2.4 ppm and, ($\triangle$) ~ 1.5 ppm signal linewidths at half-height as function of temperature in frozen 0.1 M PA in D_2O.

References

1- Yang, C.; Sharp, K. A. *Proteins* **2005**, *59*, 266.

2- Wolfe, J.; Bryant, G.; Koster, K. L. *CryoLetters* **2002**, *23*, 157.

3- Fukuhara, M.; Kokuta, A. *CryoLetters* **2005**, *26*, 251.

4- Karcher, B.; Koop, T. *Atmos. Chem. Phys.* **2005**, *5*, 703.

5- Hamdami, N.; Monteau, J. Y.; Le Bail, A. *J. Food Eng.* **2004**, *62*, 373.

6- Dash, J. G.; Fu, H. Y.; Wettlaufer, J. S. *Reports On Progress in Physics* **1995**, *58*, 115.

7- Boxe, C. S.; Colussi, A. J.; Hoffmann, M. R.; Perez, I. M.; Murphy, J. G.; Cohen, R. C. *J. Phys. Chem. A* **2006**, *110*, 3578.

8- Cho, H.; Shepson, P. B.; Barrie, L. A.; Cowin, J. P.; Zavery, R. *J. Phys. Chem.* **2002**, *106*, 11226.

9- Richardson, C. *J. Glaciol.* **1976**, *17*, 507.

10- Boxe, C. S.; Colussi, A. J.; Hoffmann, M. R.; Tan, D.; Mastromarino, J.; Sandholm, S. T.; Davies, D. D. *J. Phys. Chem. A* **2003**, *107*, 11409.

11- Schreiber, A.; Ketelsen, I.; Findenegg, G. H. *Phys. Chem. Chem. Phys.* **2001**, *3*, 1185.

12- Yeh, Y.; Feeney, R. E. *Chem. Rev.* **1996**, *96*, 601.

13- Wettlaufer, J. S.; Worster, M. G. *Annu. Rev. Fluid Mech.* **2006**, *38*, 427.

14- Henson, B. F.; Voss, L. F.; Wilson, K. R.; Robinson, J. M. *J. Chem. Phys.* **2005**, *123*, 144707.

15- Henson, B. F.; Robinson, J. M. *Phys. Rev. Lett.* **2004**, *92*, 246107.
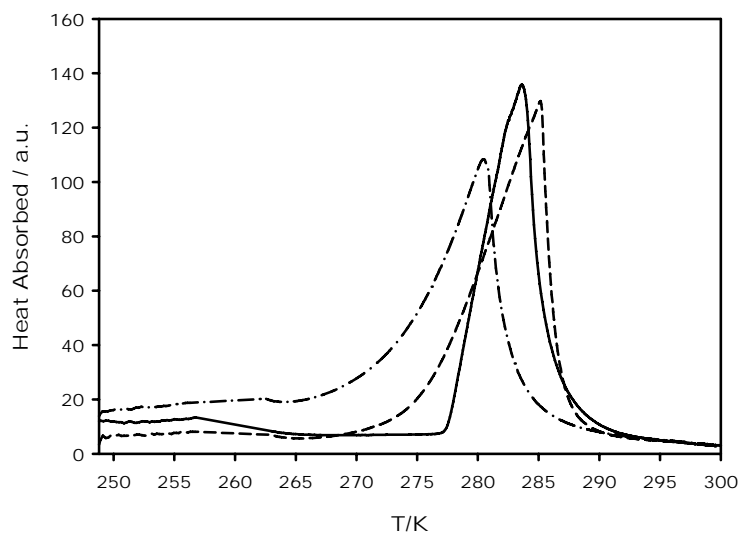
16- Ewing, G. E. *J. Phys. Chem. B* **2004**, *108*, 15953.

17- Colussi, A. J.; Hoffmann, M. R.; Tang, Y. *Langmuir* **2000**, *16*, 5213.

18- Jungwirth, P.; Vrbka, L. *Phys. Rev. Lett.* **2005**, *95*, 148501.

19- Angell, C. A. Supercooled water. In *Water, a Comprehensive Treatise*; Franks, F., Ed.; Plenum: New York, **1982**; Vol. 7.

20- Doppenschmidt, A.; Butt, H.-J. *Langmuir* **2000**, *16*, 6709.

21- Petrenko, V. F.; Whitworth, R. W. *The Physics of Ice*; Oxford University Press: Oxford, **1999**.

22- Ruzicka, R.; Barakova, L.; Klan, P. *J. Phys. Chem. B* **2005**, *109*, 9346.

23- Heger, D.; Jirkovský, J.; Klán, P. *J. Phys. Chem. A* **2005**, *109*, 6702.

24- Workman, E. J.; Reynolds, S. E. *Phys. Rev.* **1950**, *78*, 1950.

25- Finnegan, W.; Pitter, R.; Hinsvark, B. *J. Coll. Interfac. Sci.* **2001**, *242*, 373.

26- Takenaka, N.; Ueda, A.; Maeda, Y. *Nature* **1992**, *358*, 736.

27- Bronshteyn, V. L.; Chernov, A. A. *J. Crystal Growth* **1991**, *112*, 129.

28- Pincock, R. E. *Acc. Chem. Res.* **1969**, *2*, 97.

29- Takenaka, N.; Ueda, A.; Daimon, T.; Bandow, H.; Dohmaru, T.; Maeda, Y. *J. Phys. Chem.* **1996**, *100*, 13874.

30- Robinson, C.; Boxe, C. S.; Guzman, M. I.; Colussi, A. J.; Hoffmann, M. R. *J. Phys. Chem. B* **2006**, *110*.

31- Pocker, Y.; Meany, J. E.; Nist, B. J.; Zadorojn, C. *J. Phys. Chem.* **1969**, *73*, 2879.

32- Knoche, W.; Lopez-Quintela, M. A.; Weiffen, J. *Ber. Bunsenges. Phys. Chem.* **1985**, *89*, 1047.

33- Buschmann, H. J.; Dutkiewicz, E.; Knoche, W. *Ber. Bunsenges. Phys. Chem.* **1982**, *86*, 129.

34- Buschmann, H. J.; Fuldner, H. H.; Knoche, W. *Ber. Bunsenges. Phys. Chem.* **1980**, *84*, 41.

35- Menzel, H. M. *Ber. Bunsenges. Phys. Chem.* **1974**, *78*, 89.

36- Wolfe, S.; Kim, C. K.; Yang, K.; Weinberg, N.; Shi, Z. *J. Am. Chem. Soc.* **1995**, *117*, 4240.

37- Wolfe, S.; Shi, Z.; Yang, K.; S., R.; Weinberg, N.; Kim, C. K. *Can. J. Chem.* **1998**, *76*, 114.

38- Hsieh, Y. H.; Weinberg, N.; Yang, K.; Kim, C. K.; Shi, Z.; Wolfe, S. *Can. J. Chem.* **2005**, *83*, 769.

39- Likar, M. D.; Taylor, R. J.; Fagerness, P. E.; Hiyama, Y.; Robins, R. H. *Pharm. Res.* **1993**, *10*, 75.

40- Van Geet, A. L. *Anal. Chem.* **1970**, *42*, 679.

41- Angell, C. A.; Shuppert, J.; Tucker, J. C. *J. Phys. Chem.* **1973**, *77*, 3092.

42- Wong, M.; Thomas, J. K.; Nowak, T. *J. Am. Chem. Soc.* **1977**, *99*, 4730.

43- Simorellis, A. K.; Van Horn, W. D.; Flynn, P. F. *J. Am. Chem. Soc.* **2006**, *128*.

44- Thompson, K. F.; Gierasch, L. M. *J. Am. Chem. Soc.* **1984**, *106*, 3648.

45- Hansen, R. S.; Miller, F. A.; Christian, S. D. *J. Phys. Chem.* **1955**, *59*, 391.

46- Clegg, S. L.; Seinfeld, J. H.; Brimblecombe, P. *J. Aerosol Sci.* **2001**, *32*, 713.

47- Raatikainen, T.; Laaksonen, A. *Atmos. Chem. Phys.* **2005**, *5*, 2475.

48- Koop, T. *Bull. Chem. Soc. Jpn.* **2002**, *75*, 2587.

49- Johari, G. P.; Fleissner, G.; Hallbrucker, A.; Mayer, E. *J. Phys. Chem.* **1994**, *98*, 4719.

50- Koop, T.; Luo, B.; Tsias, A.; Peter, T. *Nature* **2000**, *406*, 611.

51- Steiner, T. *Angew. Chem. Int. Ed.* **2002**, *41*, 48.

52- Collins, M. D.; Hummer, G.; Quillin, M. L.; Mathews, B. W.; Gruner, S. M. *Proc. Natl. Acad. Sci. USA* **2005**, *102*, 16668.

53- Dashnau, J. L.; Sharp, K. A.; Vanderkooi, J. M. *J. Phys. Chem. B* **2005**, *109*, 24152.

54- Agreiter, J.; Frankowski, M.; Bondybey, V. *Low Temp. Phys.* **2001**, *27*, 890.

55- Gutowsky, H. S.; Holm, C. H. *J. Chem. Phys.* **1956**, *25*, 1228.

56- Krishnan, V. V.; Lau, E. Y.; Tsvetkova, N. M.; Feeney, R. E.; Fink, W. H.; Yeh, Y. *J. Chem. Phys.* **2005**, *123*, 044702.

57- Skalicky, J. J.; Sukuruman, D. K.; Mills, J. L.; Szyperski, T. *J. Am.Chem. Soc.* **2000**, *122*, 3230.

Supporting Information

Endotherms upon warming (at 0.25 K min^{-1}) previously frozen samples. Solid line:

D$_2$O ice. Dashed line: 0.1 M PA in D$_2$O. Dash-dot-dashed line: 1 M PA in D$_2$O.

Figure 3-7